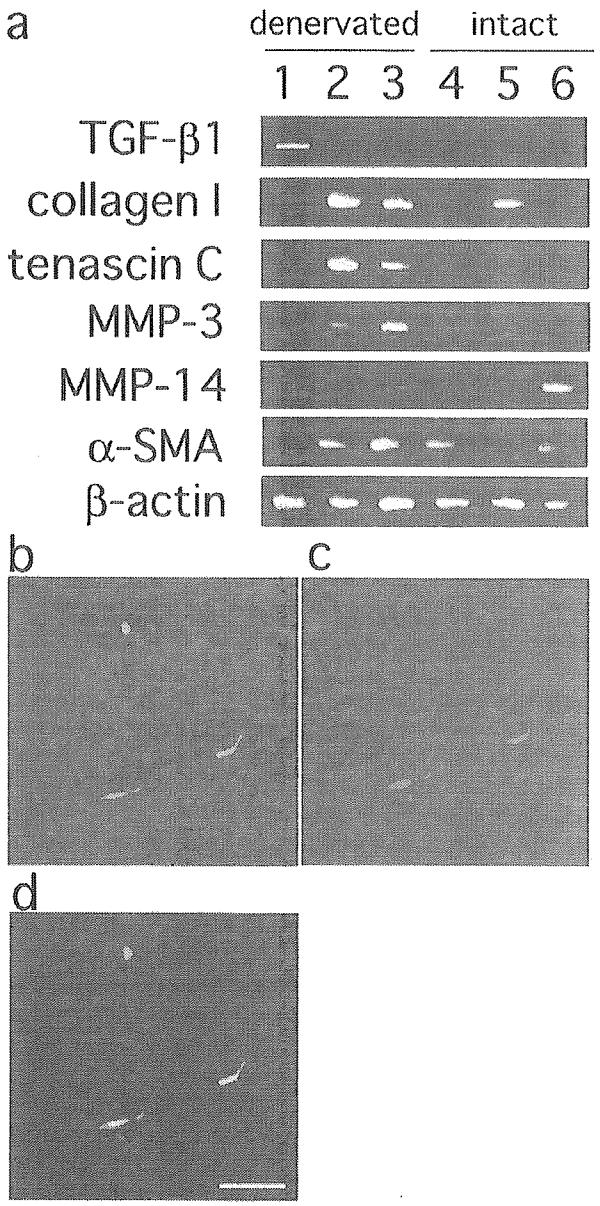

Figure 7. Expression patterns of fibrosis-related molecules within increased mononuclear interstitial cells in denervated muscle. **a:** RT-PCR analysis of fibrosis-related molecules of increased mononuclear interstitial cells in denervated muscle fractionated by FACS. Mononuclear interstitial cells were isolated from gastrocnemius muscle from either four mice 28 days after the denervation or intact mice. After appropriate immunostaining, approximately 1×10^4 cells in each fraction of GFP positive (**lanes 1** and **4**), GFP negative/CD44 positive (**lanes 2** and **5**), and GFP negative/CD44 negative (**lanes 3** and **6**) were collected by flow cytometry (corresponding to upper right, upper left, and lower left fractions in Figure 6c, respectively). After mRNA extraction from collected cells, RT-PCR was performed. Denervated mice (**lanes 1** to **3**), intact mice (**lanes 4** to **6**). **b** to **d:** Immunohistochemical detection of TGF-β1 protein in day 28 denervated gastrocnemius muscle. A portion of GFP-positive cells (**b**; green) co-stained with TGF-β1 at their cytoplasm (**c**; red) and therefore revealed a merged expression pattern (**d**; merged into yellow). Scale bars = 40 μm.

of substrates including gelatin, was expressed in the denervated muscle. MMP-3 is known to activate morphogenesis,[30] epithelial-to-mesenchymal conversion,[31] and carcinogenesis[32] of the mammary gland. MMP-3 was clearly detected in the denervated side especially in CD44-negative fraction (Figure 7a, lane 3). Although MMP-14 is reported to interact with CD44 on migrating cells,[27] less amplification of MMP-14 was detected in denervated muscle than in intact muscle. Further paradoxically, MMP-14 tended to be expressed in CD44-negative fraction (Figure 7a, lanes 3 and 6).

In MT-DCs of intact muscle, α-SMA was mainly expressed by CD44-negative fraction, probably reflecting vascular wall cells (Figure 7a, lane 6). In denervated muscle, both CD44-positive and -negative fractions showed up-regulation of α-SMA. This result may indicate an enhanced myofibroblastic phenotype in MT-DCs due to denervation, although α-SMA was not detected well among them immunohistochemically (Figure 7a, lanes 2 and 3). In denervated muscle, BM-DCs did not express α-SMA (Figure 7a, lane 1). Interestingly, BM-DCs did express α-SMA in intact muscle (Figure 7a, lane 4). Because BM cells were injected intravenously when establishing BM chimera, some of them, especially those that potentially express α-SMA, might have inappropriately homed into skeletal muscle. Therefore, such α-SMA-positive cells might, if small in number, occupy considerable proportion of BM-DCs in intact muscle, whereas α-SMA-negative migrant monocytes/macrophages might account for the majority of BM-DCs in denervated muscle. Thus, α-SMA may have been detected from BM-DCs in intact muscle and not in denervated muscle by analyzing the equal number of cells.

On the innervated side, very slight amplification of TGF-β1 expressed by BM-DCs was observed (Figure 7a, lane 4). Slight to moderate amplifications of type I collagen and tenascin-C were also observed in CD44-positive and -negative populations (Figure 7a, lanes 5 and 6). These signals may in general reflect the baseline or normal expressions of these genes.

Discussion

In this study, we proved that a great number of BM-DCs accounted for the increased number of interstitial cells in denervated skeletal muscle, in contrast to a previous study,[3] which concluded that the increased interstitial cells were derived from muscle tissue. In the experiment, white blood cell precursors were pre-labeled by repeated injection of titrated thymidine ([^{3}H]TdR) into subcutis of 7-to 10-week-old male albino mice 6 or 2 days before denervation. Determination of the presence of labeled leukocytes in denervated and control muscles was made 3 or 4 days after denervation by scintillation counting of muscle homogenates. As a consequence, incorporation of circulating-in cells into denervated extensor digitorum longus seemed unlikely in their study, although one of their time points of sampling was similar to one of those in our present study (day 4), on which an increased number of BM-DCs was observed. In contrast, bone marrow-chimeric animal enabled us to directly label bone marrow cells including mesenchymal stem cells and hematopoietic stem cells, to label peripheral leukocytes sufficiently, and to identify individual labeled cells. Thus, the negative result in the previous study for incorporation of BM-DCs

into denervated muscle may be due to technical limitations in labeling peripheral blood cells by radioisotopes or in detecting them.

Although the increased interstitial cells in denervated muscle have been currently identified as fibroblasts by electron microscopy, further intensive comparison of electron-microscopic images with that of the serial GFP fluorescent sections or immuno-electron microscopic study might enable observation of a distinction between BM-DCs and MT-DCs, bringing a novel morphological identification of these populations.

Evidence is emerging that BM-DCs play significant roles in fibrosis of other organs after progressive inflammation or injury. In pulmonary fibrosis, the majority of collagen-producing fibroblasts turned out to be bone marrow derived.[13,33] In renal fibrosis, about 14% to 15% of fibroblasts were bone marrow-derived,[12] in addition to the bone marrow monocytes that contribute to the growing process of fibrosis by facilitating the epithelial-mesenchymal transition.[34] In liver fibrosis, BM-DCs accounted for up to 22.2% of myofibroblasts: cells positive for α-SMA and vimentin and negative for CD45.[35]

In contrast, our results suggested that BM-DCs in denervated skeletal muscle were of a monocyte/macrophage lineage and therefore were not fibroblasts by definition of lineage-specific cell surface antigen, whereas that MT-DCs might contain fibroblasts. Thus, BM-DCs in denervated muscle were revealed not to differentiate into fibroblasts, as reported in fibrosis of some vital organs, but instead to maintain their monocyte/macrophage lineage. This inconsistency in the role of BM-DCs can be explained by the possibility that the pathology of denervated skeletal muscle is different from that of progressive inflammation in response to tissue injury. The increased interstitial cells in denervated muscle exhibited an anatomically characteristic distribution: they accumulated in perisynaptic regions of the denervated muscle. Interestingly, not only this accumulation but also the increase of interstitial cells itself is absent when the muscle is only immobilized by blocking the motor nerve with tetrodotoxin.[36] In addition, expression of tenascin-C or fibronectin is also undetected in such immobilized muscles.[36] These observations suggest that some signals related to denervation itself trigger the chemotaxis of macrophages to perisynaptic regions. These alterations may include axon degeneration, morphological alterations of Schwann cells around nerve terminals (terminal Schwann cells), and the lack of any substance usually supplied to the NMJ by axonal transport (Figure 8). One of the candidates for the signal factor may be monocyte chemoattractant protein-1 (MCP-1), a prototype of the CC chemokine. Mitigation of fibrosis by inhibiting monocyte infiltration with an MCP-1-blocking antibody or recently, by genetic intervention in the MCP-1 gene have been described in kidney,[37] lung,[38] and blood vessel.[39] Furthermore , MCP-1 is known to be produced by Schwann cells of denervated peripheral nerves and to induce infiltration by macrophages.[40] In denervated muscle, MCP-1 may be restrictedly expressed by terminal Schwann cells around

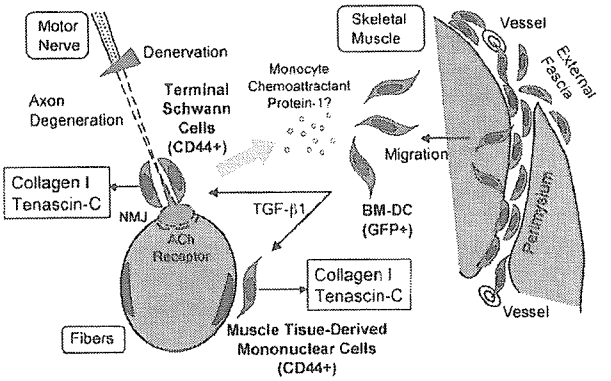

Figure 8. The cellular and molecular mechanisms of fibrosis in denervated skeletal muscle. Denervation-related signals (axon degeneration or cessation of axonal transport, for example) trigger release of chemokines such as MCP-1 from terminal Schwann cells. Circulating cells of macrophage/monocyte lineage originating from bone marrow (BM-DCs) are attracted by them and migrate to the perisynaptic region. The BM-DC release TGF-β1 to stimulate local (muscle tissue-derived) cells including fibroblasts or terminal Schwann cells to produce ECMs including type I collagen or tenascin-C. These ECMs might essentially support preservation of the position of each NMJ or induction of regenerating axons when reinnervated, although an excess of ECMs lead to fibrosis.

the perisynaptic region and may attract BM-DCs of macrophage/monocyte lineage (Figure 8).

We also showed for the first time the gene expression patterns of increased mononuclear interstitial cells in denervated skeletal muscle after dividing them into BM-DCs and MT-DCs by flow cytometric analysis. In contrast to fibrotic changes in some vital organs, BM-DCs never expressed components of ECMs, including type I collagen, in denervated muscle, whereas MT-DCs can be a main source of these ECMs. Instead, BM-DCs dominantly expressed TGF-β1, suggesting the regulatory role of BM-DCs in the fibrotic process (Figure 8). Although cultured fibroblasts isolated from denervated muscle were reported to express tenascin-C, those fibroblasts acquired the potential to produce it.[6] In addition, those "fibroblasts" might have contained other kinds of cells, including BM-DCs.

To determine functions of MT-DCs, we tried to clarify gene expression patterns of mononuclear interstitial cells by analyzing CD44-positive MT-DCs. Although all visible nerves and vessels, as shown in Figure 6, g and k, were removed before the samples were processed, immunohistochemical analysis suggested that the CD44-positive fraction possibly contained Schwann cells. One possible function of CD44 on Schwann cells is regulation of withdrawal of the myelin sheath from degenerated axons. The other possibility is that CD44 may support the connection of Schwann cells, especially perisynaptic ones (terminal Schwann cells), to muscle fibers at the position of the NMJ before denervation. This possibility may include the idea that Schwann cells also express type I collagen or tenascin-C themselves to hold their positions when denervated (Figure 8).

In the denervated side, not only the CD44-positive population but also the CD44-negative population expressed both type I collagen and tenascin-C, although these components of ECMs were more clearly detected in the CD44-positive population than in the CD44-nega-

tive population. Thus, the CD44-negative population may contain populations reactive to denervation. These may include muscle spindle cells, smooth muscle cells, vascular pericytes, perineural cells, and satellite cells. Some of these cells may express those components of ECMs or specifically express MMP-3 when denervated.

In conclusion, bone marrow-derived cells are suggested to regulate the pathogenetic process of fibrosis in denervated skeletal muscle. We believe that further investigation of the nature of BM-DCs will provide a novel approach that may lead to establishment of therapeutic amelioration of excessive fibrosis not only of denervated skeletal muscle but also of fatal neuromuscular disorders including amyotrophic lateral sclerosis as well as the latest investigations of fibrosis in other vital organs.

Acknowledgments

We are grateful to colleagues in our laboratory, in particular Dr. S. Fukada, for useful discussion and suggestions on this work.

References

1. McGeachie J, Allbrook D: Cell proliferation in skeletal muscle following denervation or tenotomy. Cell Tiss Res 1978, 193:259–267
2. Murray MA, Robbins N: Cell proliferation in denervated muscle: time course, distribution and relation to disuse. Neuroscience 1982, 7:1817–1822
3. Murray MA, Robbins N: Cell proliferation in denervated muscle: identify and origin of dividing cells. Neuroscience 1982, 7:1823–1833
4. Connor EA, McMahan UJ, Marshall RM: Cell accumulation in the junctional region of denervated muscle. J Cell Biol 1987, 104:109–120
5. Sanes JR, Schachner M, Covault J: Expression of several adhesive macromolecules (N-CAM, L1, tenascin (J1), NILE, uvomorulin, laminin, fibronectin, and a heparan sulfate proteoglycan) in embryonic, adult, and denervated adult skeletal muscle. J Cell Biol 1986, 102:420–431
6. Gatchalian CL, Schachner M, Sanes JR: Fibroblasts that proliferate near denervated synaptic sites in skeletal muscle synthesize the adhesive molecules tenascin (J1), N-CAM, fibronectin, and a heparan sulfate proteoglycan. J Cell Biol 1989, 108:1873–1890
7. Pereira RF, Halford KW, O'Hara MD, Leeper DB, Sokolov BP, Pollard MD, Bagasra O, Prockop DJ: Cultured adherent cells from marrow can serve as long-lasting precursor cells for bone, cartilage, and lung in irradiated mice. Proc Natl Acad Sci USA 1995, 92:4857–4861
8. Zhou S, Schuetz JD, Bunting KD, Colapietro AM, Sampath J, Morris JJ, Lagutina I, Grosveld GC, Osawa M, Nakauchi H, Sorrentino BP: The ABC transporter Bcrp1/ABCG2 is expressed in a wide variety of stem cells and is a molecular determinant of the side-population phenotype. Nat Med 2001, 7:1028–1034
9. Ferrari G, De Angelis GC, Coletta M, Paolucci E, Stornaiuolo A, Cossu G, Mavilio F: Muscle regeneration by bone marrow-derived myogenic progenitors. Science 1998, 279:1528–1530
10. Gussoni E, Soneoka Y, Strickland CD, Buzney EA, Khan MK, Flint AF, Kunkel LM, Mulligan RC: Dystrophin expression in the mdx mouse restored by stem cell transplantation. Nature 1999, 401:390–394
11. Sata M, Saiura A, Kunisato A, Tojo A, Okada S, Tokuhisa T, Hirai H, Makuuchi M, Hirata Y, Nagai R: Hematopoietic stem cells differentiate into vascular cells that participate in the pathogenesis of atherosclerosis. Nat Med 2002, 8:403–409
12. Iwano M, Plieth D, Danoff TM, Xue C, Okada H, Neilson EG: Evidence that fibroblasts derive from epithelium during tissue fibrosis. J Clin Invest 2002, 110:341–350
13. Hashimoto N, Jin H, Liu T, Chensue SW, Phan SH: Bone marrow-derived progenitor cells in pulmonary fibrosis. J Clin Invest 2004, 113:243–252
14. Okabe M, Ikawa M, Kominami K, Nakanishi T, Nishimune Y: 'Green mice' as a source of ubiquitous green cells. FEBS Lett 1997, 407:313–319
15. Mueller M, Leonhard C, Wacker K, Ringelstein EB, Okabe M, Hickey WF, Kiefer R: Macrophage response to peripheral nerve injury: the quantitative contribution of resident and hematogeneous macrophages. Lab Invest 2003, 83:175–185
16. Talts JF, Eng H, Zhang HY, Faissner A, Ekblom P: Characterization of monoclonal antibodies against tenascin-C: no apparent effect on kidney development in vitro. Int J Dev Biol 1997, 41:39–48
17. Savolainen J, Myllyla V, Myllyla R, Vihko V, Vaananen K, Takala TE: Effects of denervation and immobilization on collagen synthesis in rat skeletal muscle and tendon. Am J Physiol 1988, 254:R897–R902
18. Chiquet-Ehrismann R: Tenascins, a growing family of extracellular matrix proteins. Experientia 1995, 51:853–862
19. LaBarge MA, Blau HM: Biological progression from adult bone marrow to mononucleate muscle stem cell to multinucleate muscle fiber in response to injury. Cell 2002, 111:589–601
20. Ojima K, Uezumi A, Miyoshi H, Masuda S, Morita Y, Fukase A, Hattori A, Nakauchi H, Miyagoe-Suzuki Y, Takeda S: Mac-1^{low} early myeloid cells in the bone marrow-derived SP fraction migrate into injured skeletal muscle and participate in muscle regeneration. Biochem Biophys Res Commun 2004, 321:1050–1061
21. Strutz F, Okada H, Lo CW, Danoff T, Carone RL, Tomaszewski JE, Neilson EG: Identification and characterization of a fibroblast marker: FSP1. J Cell Biol 1995, 130:393–405
22. Aruffo A, Stamenkovic I, Melnick M, Underhill CB, Seed B: CD44 is the principal cell surface receptor for hyaluronate. Cell 1990, 61:1303–1313
23. Trowbridge IS, Lesley R, Schulte R, Hyman R, Trotter J: Biochemical characterization and cellular distribution of a polymorphic, murine cell-surface glycoprotein expressed on lymphoid tissues. Immunogenetics 1982, 15:299–312
24. Schmits R, Filmus J, Gerwin N, Senaldi G, Kiefer F, Kundig T, Wakeham A, Shahinian A, Catzavelos C, Rak J, Furlonger C, Zakarian A, Simard JJL, Ohashi PS, Paige CJ, Gutierrez-Ramos JC, Mak TW: CD44 regulates hematopoietic progenitor distribution, granuloma formation, and tumorigenicity. Blood 1997, 90:2217–2233
25. Protin U, Schweighoffer T, Jochum W, Hilberg F: CD44-deficient mice develop normally with changes in subpopulations and recirculation of lymphocyte subsets. J Immunol 1999, 163:4917–4923
26. Naot D, Sionov RV, Ish-Shalom D: CD44: structure, function, and association with the malignant process. Adv Cancer Res 1997, 71:241–319
27. Mori H, Tomari T, Koshikawa N, Kajita M, Itoh Y, Sato H, Tojo H, Yana I, Seiki M: CD44 directs membrane-type 1 matrix metalloproteinase to lamellipodia by associating with its hemopexin-like domain. EMBO J 2002, 21:3949–3959
28. Itoh Y, Takamura A, Ito N, Maru Y, Sato H, Suenaga N, Aoki T, Seiki M: Homophilic complex formation of MT1-MMP facilitates proMMP-2 activation on the cell surface and promotes tumor cell invasion. EMBO J 2001, 20:4782–4793
29. Pearson CA, Pearson D, Shibahara S, Hofsteenge J, Chiquet-Ehrismann R: Tenascin: cDNA cloning and induction by TGF-β. EMBO J 1988, 7:2977–2982
30. Wiseman BS, Sternlicht MD, Lund LR, Alexander CM, Mott J, Bissell MJ, Soloway P, Itohara S, Werb Z: Site-specific inductive and inhibitory activities of MMP-2 and MMP-3 orchestrate mammary gland branching morphogenesis. J Cell Biol 2003, 162:1123–1133
31. Lochter A, Galosy S, Muschler J, Freedman N, Werb Z, Bissell MJ: Matrix metalloproteinase stromelysin-1 triggers a cascade of molecular alterations that leads to stable epithelial-to-mesenchymal conversion and a premalignant phenotype in mammary epithelial cells. J Cell Biol 1997, 139:1861–1872
32. Sternlicht MD, Lochter A, Sympson CJ, Huey B, Rougier JP, Gray JW, Pinkel D, Bissell MJ, Werb Z: The stromal proteinase MMP3/stromelysin-1 promotes mammary carcinogenesis. Cell 1999, 98:137–146
33. Dunsmore SE, Shapiro SD: The bone marrow leaves its scar: new concepts in pulmonary fibrosis. J Clin Invest 2004, 113:180–182
34. Sato M, Muragaki Y, Saika S, Roberts AB, Ooshima A: Targeted disruption of TGF-β1/Smad3 signaling protects against renal tubulo-

interstitial fibrosis induced by unilateral ureteral obstruction. J Clin Invest 2003, 112:1486–1494
35. Forbes SJ, Russo FP, Rey V, Burra P, Rugge M, Wright NA, Alison MR: A significant proportion of myofibroblasts are of bone marrow origin in human liver fibrosis. Gastroenterology 2004, 126:955–963
36. Connor EA, Qin K, Yankelev H, DeStefano D: Synaptic activity and connective tissue remodeling in denervated frog muscle. J Cell Biol 1994, 127:1435–1445
37. Wada T, Furuichi K, Sakai N, Iwata Y, Kitagawa K, Ishida Y, Kondo T, Hashimoto H, Ishiwata Y, Mukaida N, Tomosugi N, Matsushima K, Egashira K, Yokoyama H: Gene therapy via blockade of monocyte chemoattractant protein-1 for renal fibrosis. J Am Soc Nephrol 2004, 15:940–948
38. Inoshima I, Kuwano K, Hamada N, Hagimoto N, Yoshimi M, Maeyama T, Takeshita A, Kitamoto S, Egashira K, Hara N: Anti-monocyte chemoattractant protein-1 gene therapy attenuates pulmonary fibrosis in mice. Am J Physiol Lung Cell Mol Physiol 2004, 286:L1038–L1044
39. Gosling J, Slaymaker S, Gu L, Tseng S, Zlot CH, Young SG, Rollins BJ, Charo IF: MCP-1 deficiency reduces susceptibility to atherosclerosis in mice that overexpress human apolipoprotein B. J Clin Invest 1999, 103:773–778
40. Tofaris GK, Patterson PH, Jessen KR, Mirsky R: Denervated Schwann cells attract macrophages by secretion of leukemia inhibitory factor (LIF) and monocyte chemoattractant protein-1 in a process regulated by interleukin-6 and LIF. J Neurosci 2002, 22:6696–6703

Acta Myologica • 2005; XXIV: p. 74-77

Regulation of splicing by MBNL and CELF family of RNA-binding protein

S. ISHIURA*, Y. KINO, Y. NEZU, H. ONISHI, E. OHNO, AND N. SASAGAWA

Department of Life Sciences, Graduate School of Arts and Sciences, The University of Tokyo, 3-8-1 Komaba, Meguro-ku, Tokyo, Japan 153-8902

Myotonic Dystrophy (DM), the most common form of adult-onset muscular dystrophy, comprises at least 2 subtypes, DM1 and DM2. DM1 is caused by the expansion of a CTG repeat located in the 3' untranslated region of the DM protein kinase (*DMPK*) gene. Recently, the expansion of a CCTG tetranucleotide repeat located in the first intron of the *ZNF9* gene was identified as the mutation responsible for DM2. Since both DM1 and DM2 are caused by the expansion of repetitive sequences, some common factors that interact with these sequences might be involved in the pathogenesis of DM. MBNL1 is a candidate for such factors and is thought to be sequestered by the expanded forms of DM transcripts.

Key words: myotonic dystrophy, RNA repeat, MBNL1

Myotonic dystrophy is the most common form of adult-onset muscular dystrophy [1]. It is inherited by autosomal dominant fashion. Myotonic dystrophy causes a consistent constellation of unrelated clinical features, including myotonia, cardiac conduction defects, cataracts, and specific set of endocrine changes, and so on. The underlying genetic mutation causing myotonic dystrophy is unstable expanded CTG repeat in the 3'-untranslated region of a gene on chromosome 19 encoding a DM protein kinase (DMPK) of unknown function [2]. The mutation is transcribed into RNA but not translated into protein. Recently, myotonic dystrophy type 2 (DM2) was found to be caused by a CCTG tetranucleotide expansion in intron 1 of the Zn-finger protein ZNF-9 gene on chromosome 3 [3]. DM2 is also caused by a transcribed but untranslated repeat expansion. Although DM2 is generally a milder disease than DM1, the DM2 CCTG expansions is much larger than DM1 CTG expansions.

Reddy et al. showed that DMPK knockout mice did not fully recapitulate DM. This means that loss of DMPK function is not the main cause of DM [4]. RNA inclusions of CUG/CCUG repeats are observed as foci in the nuclei of DM patients. Transgenic mice expressing CUG repeats under the skeletal muscle actin promoter showed myotonia and abnormal muscle histology [5]. In this case, the severity of phenotype was correlated with the expression level of CUG repeat RNA. These results suggest that abnormality in RNA metabolism is involved in DM [1].

The clinical features common to both DM1 and DM2 may be caused by a gain-of-function RNA mechanism in which the CUG and CCUG repeats alter cellular function by sequestering repeat RNA-binding proteins.

Two families of RNA-binding proteins

Two families of RNA repeat-binding proteins have been implicated in DM pathogenesis: CELF (CUG-BP11 and ETR-3-like factors) and MBNL(muscleblind-like) proteins. Six CELF genes have been identified in human genome and they have been shown to be involved in alternative splicing [6]. Among these, CUG-BP1 regulates alternative splicing of cardiac troponin T (cTnT), insulin receptor (IR) and chloride channel 1 (ClC-1) that are misregulated in DM muscle [7,8]. MBNL is a homologue of *Drosophila* muscleblind which is involved in the differentiation of skeletal muscle and photoreceptor [9]. Three genes (*MBNL1, 2* and *3*) are identified in humans. A mouse knockout reproduced myotonia and cataract, and misregulation of splicing was observed [10].

We investigated the in vivo binding-sequence specificity of these proteins using a yeast 3 hybrid

*Address for correspondence: correspondence should be addressed to Dr. S.Ishiura**

system [11,12]. In this assay, the association of an RNA-binding protein Y with its cognate RNA X binding site leads to the transcriptional activation of a reporter gene, such as His3 and β-galactosidase, in yeast. We generated a variety of repetitive RNA sequences and examined them.

The results are shown in Table 1. CUG-BP1 (this protein is first identified as a CUG triplet repeat-binding protein) strongly interacted with UG dinucleotide repeat [11]. Neither PKR (protein kinase R), a double stranded nucleotide-binding protein, nor CUG-BP1 interacted strongly with CUG/CCUG repeats. By contrast, MBNL1 showed apparent interactions with both CUG and CCUG repeats.

Table 1. RNA-binding specificity of candidate proteins.

Repeat	CUG-BP1	MBNL1	PKR
UG24	+++++	-	-
CA24	-	-	-
CUG7	-	-	-
CUG16	-	++	-
CUG21	-	+++	-
CUG37	-	++	-
CUG70	-	++	+
CCUG7	+	-	-
CCUG22	-	++++	-
CCUG50	-	+++	-
CAGG22	-	-	-
CAGG50	+	-	-
CGGG20	-	-	-
CCCG21	++	++++	-
UAUG7+CAUA7	-	-	+++++
CAG16+CUG16	-	-	+++++

The transformation of yeast cells and reporter gene assays were performed as previously described (11,12). We classified the binding activity as (+++++), (++++), (+++) and (++), when yeast grown was observed on the plates containing 1, 0.5, 0.1 and 0mM 3-AT, respectively. (+) yeast grew in the absence of 3-AT after more than 1 week, (-) no growth of yeast transformants was observed even after prolonged incubation.

We confirmed these results by surface plasmon resonance technique. Surface Plasmon Resonance (SPR) is a powerful technique to measure biomolecular interactions in real-time in a label free environment. Protein is immobilized to the sensor surface, and the repeat RNA is passed over the surface. Association and dissociation is measured and displayed in a graph called the sensor-gram. CUG-BP1 strongly interacted with UG-repeat but not CUG repeat, while MBNL1 interacted with CCUG repeat (data not shown). These results indicate that loss of function of MBNL1, not CUG-BP1, may be important for DM pathogenesis. Sequestration of MBNL1 by the long CUG/CCUG repeat may disrupt normal cellular function of MBNL1, which leads to abnormal phenotype of myotonic dystrophy.

Table 1 also shows that MBNL1 interacted strongly with CCCG, modestly with CUUG and CAUG, but not at all with CGGG and so on. On the other hand, PKR strongly interacted with double-stranded RNAs. All these results suggest MBNL1 binds to repeats with incomplete double strand, but not to the complete one. The deduced target sequence of MBNL1 could be CHHG or CHG repeat, where H is the nucleotide other than G. Secondary structure of CHHG repeat can be calculated as a long hairpin with mismatches. Since MBNL1 does not bind to CUG/CAG double strand repeat without mismatch, the presence of mismatch is necessary for the binding of MBNL1 to the target sequences.

To confirm the results of the three-hybrid analyses, we performed gel retardation analysis [12]. First, we fused MBNL1 with glutathione S-transferase (GST) in the N-terminus and a His-tag in the C-terminus. GST-MBNL1 was expressed in E.Coli and purified. GST-MBNL1 bound to a ^{32}P-labeled CCUG probe, and supershift was observed when an anti-GST antibody was added. The extent of band shift was reduced by adding non-labeled CCUG RNA. We also examined the dependence of the binding between CCUG repeats and MBNL1 on the repeat length. Free probes of CCUG27 and CCUG35 disappeared at the highest dose of MBNL1. The number of shifted bands represents the variety of RNA-protein complexes, mainly reflecting the number of proteins binding to a single probe.

Structure of MBNL1 and homologues

MBNL1 has at least nine splice variants. MBNL1 has four Zn finger motifs at the N-terminal half of the molecule, which may be involved in the RNA-binding. There is a nuclear localization signal at the C-terminus. Some of the isoforms of MBNL1 was localized at the nucleus. The others were in the cytosol. Therefore, MBNL1 might have many cellular functions. Furthermore, not only MBNL1 but also MBNL2 and 3 are

reported to be colocalized with RNA foci of CUG/CCUG repeats. We have determined the binding specificity of these MBNL families to various RNA repeats. MBNL2 and MBNL3 had almost similar specificity to MBNL1 (data not shown). These MBNL isoforms also showed different localization. Therefore we have to be careful for analyzing the data, because three MBNL proteins have many isoforms and these isoforms may have diverse functions in various tissues.

Regulation of alternative splicing by RNA repeat-binding proteins

Myotonic dystrophy is an example of a disease that alters the function of RNA-binding proteins to cause misregulated alternative splicing [1]. Many misregulated alternative splicing events have been demonstrated for eight pre mRNAs. In all cases, normal mRNA splice variants are produced, but the normal developmental splicing pattern is disrupted, resulting in the expression of fetal protein isoforms.

The insulin resistance and myotonia observed in DM1 correlate with the disruption of splicing of targets, IR and ClC-1. The counter regulation of mRNA splicing by the two proteins, CUG-BP1 and MBNL1 is demonstrated [9]. When cTNT mini-gene was expressed with CUG-BP1, a fetal isoform including exon 5 was predominantly expressed, while coexpression with MNBL1 suppressed the formation of the fetal isoform. In the case of insulin receptor mini-gene, MBNL1 enhanced the formation of long form with exon 11, while CUG-BP1 was not. These results suggest that these two RNA-binding proteins counteracted *in vivo*.

However, in the case of alpha-actinin, MBNL1 may not always act antagonistically against CUG-BP1s. Alpha-actinin has two exons, nonmuscle type and skeletal muscle type. These are exclusively expressed in vivo. However, in our assay system, MBNL1 does not act antagonistically against CUG-BP1. Both enhanced the production of non-muscle type (Fig.1). These data also predict that change in expression of these alternative splicing regulators would result in the splicing alterations that have been shown to be characteristic of the myotonic dystrophy. However, all targets of these proteins have never been clarified. In addition, these regulators appear to express independently.

There have been many reports that excess oxidative stress occurs in the muscle with expanded CTG repeats [13-15]. The stress accelerates an apoptotic process, leading to cell death. The increase in oxidative stress in response to expended RNA repeats is likely to involve yet unidentified signaling event that remain to be determined. Misregulation of splicing may also be evoked by the cellular signaling processes.

Acknowledgments

This work was supported in part by grants (to S.I.) from the Ministry of Health, Labor and Welfare, Japan, and the Ministry of Education, Science, Sports and Cuture, Japan.

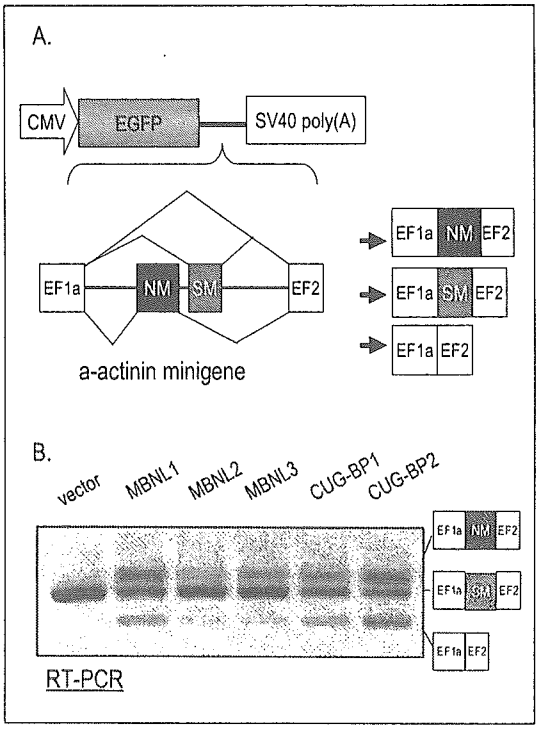

Figure 1. MBNL andCUG-BP1 promote exon skipping.

A. The α-actinin minigene contains two exons (nonmuscle type NM and smooth muscle type SM) flanked by EF1a and EF2 exons.

B. COS cells were cotransfected with the minigene and each of RNA-binding protein expression plasmid. Exon inclusion was assayed by RT-PCR.

References

1. Ranum LPW, Day JW. Myotonic dystrophy:RNA pathogenesis comes into focus. Am J Hum Genet 2004;74:793-804.
2. Sasagawa N, Ishiura S. Myotonic dystrophy protein kinase. Wiley Encyclopedia Mol Med 2002;5:2203-05.
3. Day JW, Ricker K, Jacobson JF, et al. Myotonic dystrophy type 2:molecular, diagnostic and clinical spectrum. Neurology 2003;60:657-64.
4. Reddy S, Smith DB, Rich MM, et al. Mice lacking the myotonic dystrophy protein kinase develop a late onset progressive myopathy. Nat Genet 1996;13:325-335.
5. Ladd AN, Nguyen NH, Malhotra K, Cooper TA. CELF6, a member of the CELF family of RNA-binding proteins, regulates muscle-specific enhancer-dependent alternative splicing. J Biol Chem 2004;279:17756-64.
6. Mankodi A, Logigian E, Callahan L, et al. Myotonic dystrophy in transgenic mice expressing an enpanded CUG repeat. Science 2000;289:1769-73.
7. Timchenko LT, Timchenko NA, Caskey CT, Roberts R. Novel proteins with binding specificity for DNA CTG repeats and RNA CUG repeats: implication for myotonic dystrophy. Hum Mol Genet 1996;5:1115-21.
8. Ho TH, Bundman D, Armstrong DL, Cooper TA. Transgenic mice expressing CUG-BP11 reproduce splicing mis-regulation observed in myotonic dystrophy. Hum Mol Genet 2005;14:1539-47.
9. Ho TH, Charet-B N, Poulos MG, et al. Muscleblind proteins regulate alternative splicing. EMBO J 2004;23:3103-12.
10. Kanadia RN, Johnstone KA, Mankodi A, et al. A muscleblind knockout model for myotonic dystrophy. Science 2003;302:1978-80.
11. Takahashi N, Sasagawa N, Suzuki K, Ishiura S. The CUG-binding protein (CUG-BP1) binds specifically to UG dinucleotide repeats in a yeast three-hybrid system. Biochem Biophys Res Commun 2000;277:518-23.
12. Kino Y, Oma Y, Sasagawa N, Ishiura S. Muscleblind protein, MBNL1/EXP, binds specifically to CHHG repeats. Human Mol Genet 2004;13:495-507.
13. Usuki F, Takahashi N, Sasagawa N, Ishiura S. Differential signaling pathways following oxidative stress in mutant myotonin protein kinase cDNA transfected C2C12 cell lines. Biochem Biophys Res Commun 2000;267:739-743.
14. Usuki F, Yasutake A, Umehara F, et al. In vivo protection of a water-soluble derivative of vitamin E, Trolox, against methylmercury-intoxication in the rat. Neurosci Lett 2001;304:199-203.
15. Takeshita Y, Sasagawa N, Usuki F, Ishiura S. Decreased expression of alpha-B-crystallin in C2C12 cells that express human DMPK/160CTG repeats. Basic Appl Myol 2003;13:305-8.

Available online at www.sciencedirect.com
SCIENCE DIRECT
Biochimica et Biophysica Acta 1748 (2005) 174–179
BIOCHIMICA ET BIOPHYSICA ACTA BBA
http://www.elsevier.com/locate/bba

Comparative analysis of the cytotoxicity of homopolymeric amino acids

Yoko Oma, Yoshihiro Kino, Noboru Sasagawa, Shoichi Ishiura*

Department of Life Sciences, Graduate School of Arts and Sciences, The University of Tokyo, Japan

Received 8 November 2004; received in revised form 28 December 2004; accepted 29 December 2004
Available online 27 January 2005

Abstract

Many human proteins have homopolymeric amino acid (HPAA) tracts, although the physiological significance or cellular effects of their presence is poorly understood. We previously reported that 20 kinds of HPAAs show characteristic intracellular localization and that among those, hydrophobic HPAAs aggregate strongly and form high molecular weight proteins when expressed in cultured cells. In this study, we investigated the cytotoxicity of 20 kinds of HPAAs. HPAA tracts of ~30 residues fused to the C-terminus of YFP were expressed in COS-7 cells. Cells expressing homopolymeric-Cys, -Ile, -Leu, and -Val showed low viability in Trypan Blue assay. Caspase-3 activity, which is usually upregulated in dying cells, was determined by measuring the cleavage of the peptide substrate Ac–DEVD–MCA and by detecting the cleaved active form of the caspase-3 by Western blotting. The activity of caspase-3 was drastically elevated in cells expressing those HPAAs which showed low viability in Trypan Blue assay. Interestingly, it was found that there is a correlation between the hydrophobicity of a single amino acid and the cytotoxicity of the corresponding HPAA as a homopolymer. These results indicate that the hydrophobicity of HPAAs may cause cytotoxicity.

Keywords: Polyglutamine; Polyalanine; Triplet repeat; Cell death; Cytotoxicity; Caspase

1. Introduction

Higher organisms contain thousands of protein species, whose functional diversity is based on the diversity of their components, amino acids, and their numerous combinations. Homopolymeric amino acids (HPAAs) are distinct tracts of amino acids comprising consecutive sequences of the same amino acid, some of which are often found in natural proteins [1]; HPAA tracts may either play some roles in or have effect on cells. Each HPAA has characteristic properties reflecting the diversity of amino acids. Indeed, we recently reported differential patterns of intracellular localization of HPAAs fused to YFP [2]. Moreover, several genetic diseases associated with the expansion of HPAA tracts have been reported [3–6]. Polyglutamine expansions cause several genetically inherited diseases including Huntington's disease. It has been observed that expanded polyglutamine forms neuronal intranuclear inclusions in animal models of polyglutamine diseases and in the central nervous system of patients with these diseases [7,8]. Expanded polyglutamine is thought to confer toxic properties on the disease proteins with a dominant gain-of-function that causes cell death or dysfunction. However, the role of the aggregate formation in disease pathology is not clarified yet [9–11]. Besides expanded polyglutamine, intranuclear aggregation of the causative protein with expanded polyalanine in skeletal muscle fibers is the morphological hallmark of oculopharyngeal muscular dystrophy (OPMD), one of the polyalanine diseases [12,13], suggesting a possible common mechanism between OPMD and polyglutamine diseases. Huntington's disease-like 2, a novel disease with similar symptoms to Huntington's disease, has been described as being caused by the expansion of CTG repeats, which are translated into either polyalanine or polyleucine stretches [14].

Even outside a disease-related protein context, polyglutamine or polyalanine tracts themselves have been

* Corresponding author. Fax: +81 3 5454 6739.
E-mail address: cishiura@mail.ecc.u-tokyo.ac.jp (S. Ishiura).

1570-9639/$ - see front matter © 2005 Elsevier B.V. All rights reserved.
doi:10.1016/j.bbapap.2004.12.017

studied and their expansion has been shown to confer aggregative and cytotoxic properties. For example, when GFP-fused polyglutamine tracts of 19, 35, 56, and 80 residues were expressed in primary neurons, 35, 56, and 80 residues formed aggregate(s) and 80 residues upregulated caspase activity [15]. Similarly, the expression of GFP-fused polyalanine tracts of 19, and 37 residues in COS-7 cells results in formation of aggregates with higher rates of cell death for cells containing the 19 or 37 residue constructs compared with cells containing the 0 or 7 residue constructs [16]. COS-7 cells, which we used in this study, are often used as a good cellular model of polyglutamine and polyalanine diseases since they mimic many of features of the diseases including length dependent aggregation and cell death. Polyalanine peptides 14 residues in length have been shown to form beta-sheets in vitro [17], and extended polyglutamine repeats have also been shown to form such structures in vitro and in vivo [18,19]. Apart from polyglutamine and polyalanine, polyleucine tracts of 291 residues in length have been reported to possess even stronger cytotoxicity compared to polyglutamine tracts of the same length [20]. These results suggest that the length and species of homopolymeric amino acids may produce varying cytotoxic effects.

To understand the properties of HPAAs comparatively, we previously reported the specific localizations of 20 kinds of HPAAs, and showed that hydrophobic HPAAs aggregate strongly and form high molecular weight complexes [2]. Though intracellular aggregation is limited in polyglutamine and polyalanine diseases, as mentioned above, some HPAAs other than polyglutamine or polyalanine might have cytotoxic effects. In this report, we compared the cytotoxicity of 20 kinds of HPAAs composed of 30 residues under the same experimental conditions.

2. Materials and methods

2.1. Fluorescence microscopy analysis

COS-7 cells were grown in DMEM with 10% fetal bovine serum (Sigma-Aldrich, Tokyo, Japan). Transient transfection was performed using FuGENE 6 Transfection reagent (Roche Diagnostics, Tokyo, Japan) following the manufacturer's instructions. The cells were treated with Hoechst33342 (Sigma-Aldrich, Tokyo, Japan) at 37 °C for 30 min, and the medium was removed and replaced with PBS. The fluorescence of YFP was visualized by fluorescence microscopy IX70 (Olympus, Tokyo, Japan).

2.2. Transfection efficiency

COS-7 cells were transiently transfected with the YFP–HPAA plasmid. After incubation for 48 h, the cells were harvested and dissolved in PBS. The percentage of transfected cells was determined as fluorescent positive cells by flow cytometry (EPICS® XL™, Beckman Coulter).

2.3. Trypan Blue assay

COS-7 cells were seeded at 1.2×10^4 per well in 24-well plates and were transiently transfected with 0.3 μg of YFP–HPAA plasmid after incubation for 19 h. The cells were harvested and treated with Trypan Blue (Sigma-Aldrich, Tokyo, Japan) 48 h after transfection. In each experiment, about 150 cells were examined under a microscope to determine the number of dead cells (stained) and living cells (unstained).

2.4. Caspase-3 assay

COS-7 cells were seeded at 2.0×10^5 per 35 mm dish and were transiently transfected with 0.75 μg of YFP–HPAA plasmids after incubation for 24 h. The cells were harvested and dissolved in extraction buffer (50 mM Tris–HCl, pH7.5, 10 mM 2-mercaptoethanol, 1 mM EDTA) 48 hours after transfection. The samples were subjected to three rounds of freezing in liquid nitrogen for 60 s and thawing in a 30 °C water bath for 90 s, after which the samples were centrifuged at 10,000 ×*g* for 5 min. The total protein (7.4 μg) in the supernatant was dissolved in 200 μl of assay buffer (25 mM Tris–HCl, pH7.5, 10 mM 2-mercaptoethanol, 1 mM EDTA). A fluorescent substrate for caspase-3, Ac-Asp-Glu-Val-Asp-MCA (Peptide Institute, Tokyo, Japan), was added to a final concentration of 5 μM, and the mixtures were incubated at 37 °C for 30 min. The reactions were stopped by the addition of 100 μl of 10% SDS, 1 ml of 0.1 M NaOAc, and the fluorescence was measured with a JASCO FP-777 fluorescence spectrometer (excitation, 380 nm; emission, 460 nm).

2.5. Western blot analysis

COS-7 cells were seeded at 1.5×10^5 per 60 mm dish and were transiently transfected with 2.0 μg of YFP–HPAA plasmids after incubation for 24 h. After incubation for 48 h, the cells were harvested and sonicated in PBS with 1% Triton X-100 and 0.1% protease inhibitor mix (Wako, Osaka, Japan). The protein concentration was measured with a DC protein Assay Kit (Bio-Rad laboratories, Tokyo, Japan). Equal amounts of protein, 41 μg for each sample, were subjected to SDS-polyacrylamide gel electrophoresis on 15% gels and transferred onto PVDF membranes (Finetrap NT-32; Nihon Eido, Tokyo, Japan). The membranes were incubated with Caspase 3 (8G10) rabbit monoclonal antibody (1:1000; Cell Signaling Thechnology, U.S.A.) at 4 °C for overnight, and then with anti-rabbit IgG anitibody at 37 °C for 30 min. The resulting menbranes were visualized with Enhanced

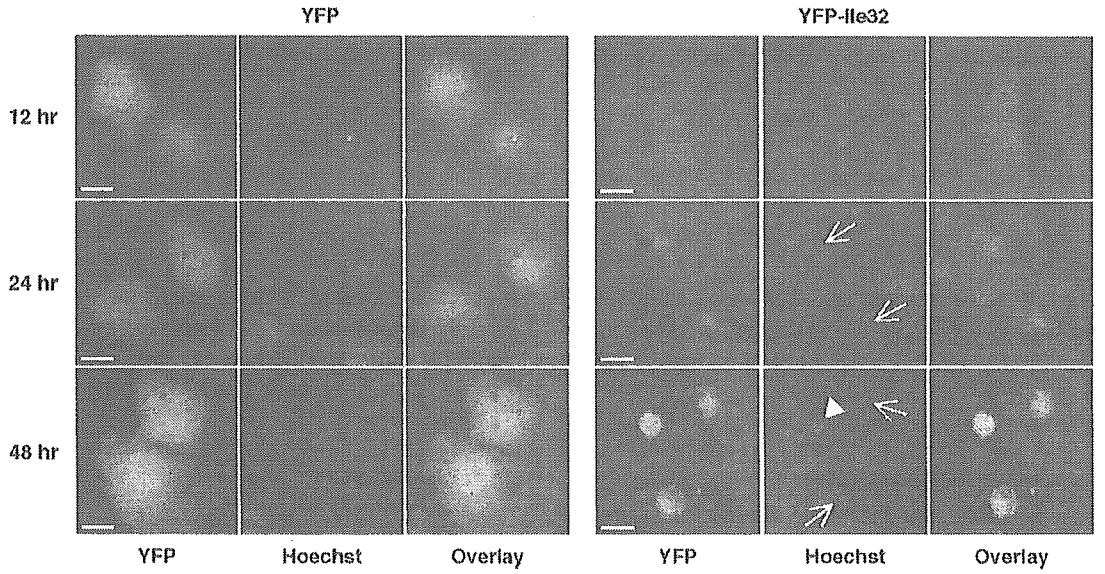

Fig. 1. The intracellular localization of YFP and YFP-fused homopolymeric-Ile32. The nuclei were stained by Hoechst. Homopolymeric-Ile32 formed one large aggregate in the perinuclear region of each cell. The nuclei of the cells expressing homopolymeric-Ile32 showed distorted morphology around the aggregates (arrow) and become aberrant (arrow head) at 48 h after transfection. Scale bar, 20 μm.

Chemiluminescence kit (Amersham Bioscience, Tokyo, Japan).

3. Results

3.1. Cell viability assay

We have previously shown that hydrophobic HPAAs aggregate strongly in COS-7 cells [2]. Fig. 1 shows the intracellular localization of YFP-fused homopolymeric-Ile32, one of the typical aggregate-forming HPAAs. The nuclei of the cells expressing homopolymeric-Ile32 were stained by Hoechst, and showed distorted morphology around the aggregates (arrow) and became aberrant (arrow-head) at 48 h after transfection. We observed many floating cells expressing Ile32, but not YFP only, suggesting that cell death is caused by the expression of this HPAA.

To study the effects of HPAAs on cells, we performed cell viability assays by staining dead cells with Trypan Blue. Twenty HPAAs, each comprising approximately 30 residues (26~32) fused to the C-terminus of YFP, were expressed in COS-7 cells. Forty-eight hours after transfection, we treated cells with Trypan Blue and determined the ratio of stained (dead) cells to unstained (living) cells. The transfection efficiency was examined and there was no significant difference among all constructs on analysis of variance (ANOVA) tests (data not shown). Compared to cells expressing only YFP, cells expressing YFP-fused homopolymeric-Ile, -Cys, -Val, and -Leu showed significantly low viability followed by cells expressing homopolymeric-Phe, -Trp, -Met, and -Ala (Fig. 2).

3.2. Caspase-3 assay

Caspase-3 activity is known to rise at the very downstream point of apoptotic cell death [21]. Forty-eight hours after transfection we assessed the caspase-3 activity by measuring the cleavage of the peptide substrate Ac-DEVD-MCA. Longer HPAAs (Ala70, Gln150) induced higher caspase-3 activities than their shorter counterparts (Fig. 3A), which is consistent with the previous reports that long

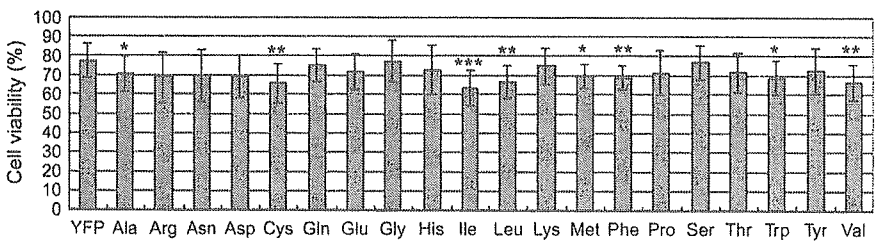

Fig. 2. Cell viability assay. Cell viability was measured 48 h after transfection by Trypan Blue assay. Compared to cells expressing only YFP, cells expressing YFP-fused homopolymeric-Ala, -Cys, -Ile, -Leu, -Met, -Phe, -Trp, and -Val showed low viability. Student's *t* Test was performed with the control (only YFP). *$p<0.05$; **$p<0.01$; ***$p<0.001$; Mean±S.D.; $n=10$.

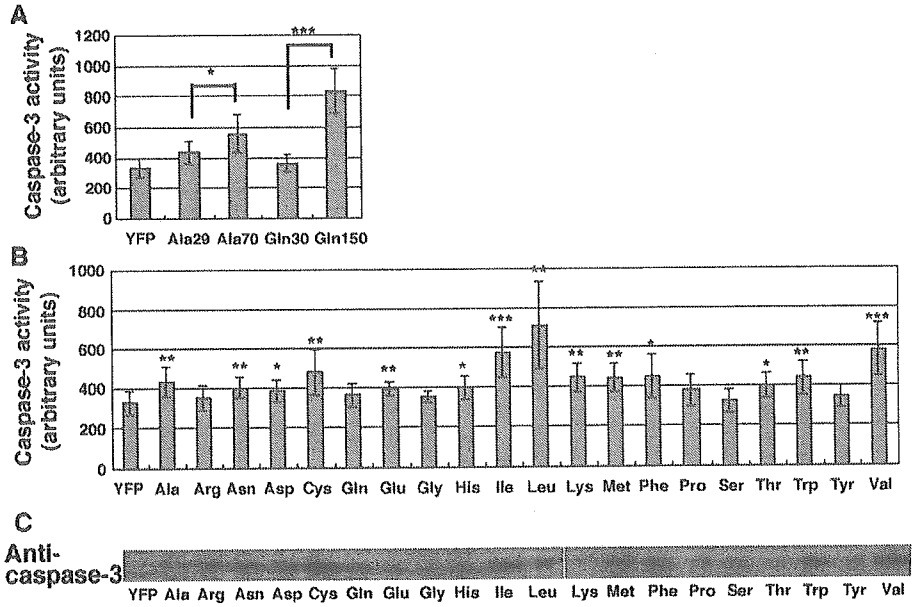

Fig. 3. Caspase-3 assay. Caspase-3 activity was measured 48 h after transfection. (A) Caspase-3 activity was upregulated when longer stretches of polyglutamine (150 residues) or polyalanine (70 residues) were expressed compared to shorter stretches (30 residues). (B) Compared to cells expressing only YFP, cells expressing YFP-fused homopolymeric-Leu, -Val, -Ile, -Cys, followed by -Phe, -Lys and -Met, showed high caspase-3 activities. Student's *t* Test was performed with the control (only YFP). $*p<0.05$; $**p<0.01$; $***p<0.001$; Mean±S.D.; $n=9$ (C) The cleaved active fragment of caspase-3 was detected by Western blot analysis with anti-caspase-3 antibody.

polyglutamine and polyalanine tracts have cytotoxic effects [15,16]. Among the 20 HPAAs comprising 30 residues, a drastic upregulation of caspase-3 occurred in cells expressing homopolymeric-Leu, -Val, -Ile, and -Cys compared with control cells expressing only YFP, suggesting that these HPAAs have strong cytotoxic effects (Fig. 3B). Homopolymeric-Leu produced the highest upregultion of caspase-3, followed by -Val, -Ile, and -Cys. Some other HPAAs, homopolymeric-Ala, -Asn, -Asp, -Glu, -His, -Lys, -Met, -Phe, -Thr, and -Trp, also produced significantly elevated caspase-3 activities. Next, the cleaved active fragment of the caspase-3 (17/19 kDa) was measured by Western blotting with an anti-caspase 3 antibody (Fig. 3C). Cells expressing homopolymeric-Asn, -Asp, -Cys, -Ile, -Leu, -Met, -Phe, -Trp, and -Val showed an increased amount of cleaved active fragment of caspase-3, which is approximately consistent with our caspase-3 assay shown in Fig. 3B. The same experiment was repeated three times and similar results were observed each time (data not shown).

The results of the cell viability assay and the caspase-3 assay declared cytotoxicity of several HPAAs, especially homopolymeric-Cys, -Ile, -Leu and -Val. HPAAs which showed cytotoxicity in these assays seem to be hydrophobic HPAAs. We plotted the cytotoxicity of each HPAA as measured in these experiments, the hydrophobicity of each amino acid [22] versus cell viability and caspase-3 activity

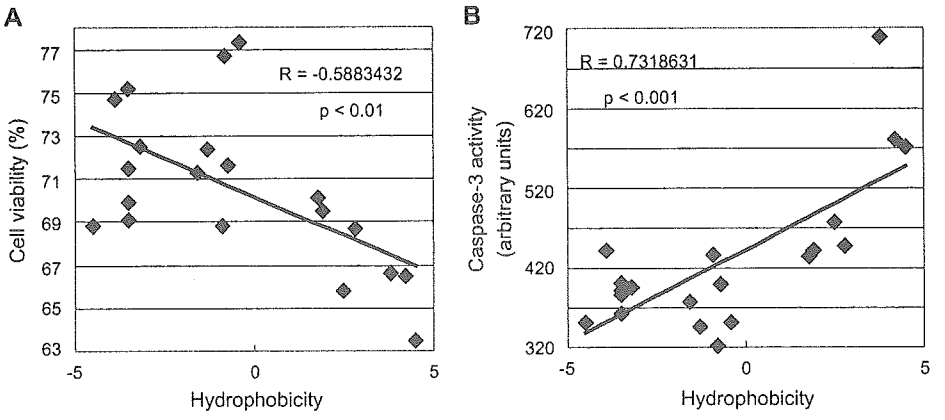

Fig. 4. Cytotoxicity and hydrophobicity. There is a correlation between the level of cytotoxicity of an HPAA and the hydrophobicity of its amino acid. Hydrophobicity of each amino acid as calculated in ref.22 was plotted versus the cytotoxicities of HPAAs measured by (A) the cell viability assay and, (B) the caspase-3 activity assay.

(Fig. 4A and B, respectively). As shown in the plot, there is a significant correlation between the cytotoxicity of an HPAA and the hydrophobicity of its amino acid, indicating that the higher hydrophobic properties of a protein might induce more severe toxicity in cells.

4. Discussion

There are many proteins containing various kinds of HPAAs, and several diseases are caused by the expansions of such amino acid repeats, including polyglutamine and polyalanine. This is the first report which investigated cytotoxicity of not only polyglutamine, polyalanine, or polyleucine but also other HPAAs, all 20 kinds of HPAAs comparatively.

To investigate the effect of all 20 HPAAs in cells, we performed two assays, cell viability assay and caspase-3 activity assay, to detect the cytotoxicity of HPAAs expressed in cells. Our results suggest that among all HPAAs, homopolymeric-Cys and hydrophobic HPAAs such as homopolymeric-Ile, -Leu, and -Val, tend to have highly toxic effects in cells. And there was a correlation between the cytotoxicity of an HPAA and the hydrophobicity of its amino acid, indicating that the higher hydrophobic properties of a protein might induce more severe toxicity in cells. Interestingly, we previously showed that these hydrophobic HPAAs aggregate strongly and form high molecular weight proteins [2]. Therefore, our results suggest that aggregation-prone proteins may have cytotoxicity. Importantly, there is a bias in the distribution of HPAA species, so that hydrophobic HPAAs are rare in natural proteins. In the previous report, we predicted that the scarcity of these HPAAs might derive from their cytotoxicity since those HPAAs aggregate strongly in cells. In this report, we demonstrated the plausibleness of the prediction that HPAAs which aggregate in cells have cytotoxicic effect and might be less abundant in natural proteins. Fig. 5 depicts a diagram of 20 amino acids situated according to their properties with the red circle showing cytotoxicity as revealed in our study. Aliphatic hydrophobic HPAAs and homopolymeric-Cys showed the most significant toxicity in our assays.

The accumulation of altered proteins is a common pathogenic mechanism in several neurodegenerative disorders including polyglutamine diseases, Alzheimer's disease, and Parkinson's disease [9,23]. Although there must be specific mechanisms for each disease according to the responsible protein, aggregate formation itself might have significant relation with toxicity [24]. It has been suggested that the soluble oligomers of these proteins are crucial to the toxic mechanism rather than the subsequent aggregates or fibrils [25]. The role of aggregation or oligomerization is a very important issue for solving the mechanism of the cytoxicity of these proteins. It has been reported that protein aggregation directly impairs the function of the ubiquitin–proteasome system [26] or causes an unfolded protein

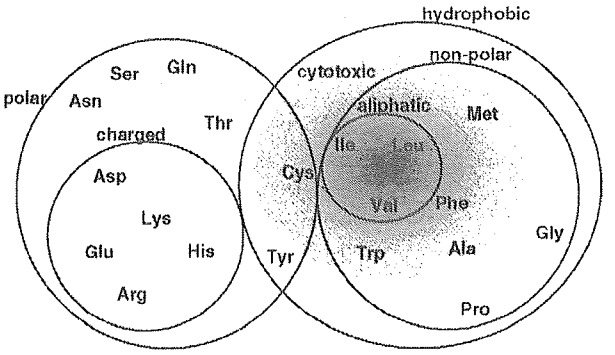

Fig. 5. Properties of single amino acids and the cytotoxicity of their homopolymers. The diagram shows the relationship among 20 amino acids in terms of their properties. Cytotoxic HPAAs are within the red circle.

response [27]. Recently, it has also been reported that endoplasmic reticulum (ER) stress is caused by the accumulation of unfolded and malfolded proteins, including amyloid beta peptide in Alzheimer's diseases [28], polyglutamine-containing proteins [29,30] and prion protein [31].

Here, we show the cytotoxicities of hydrophobic HPAAs in cultured cells, thus confirmed the previous prediction that hydrophobicity of HPAAs might be an important determinant of cytotoxicity as well as aggregation. Furthermore, our system using various kinds of HPAAs not only reveals the specific properties of each HPAA, but also can be used as a model of aggregation-prone proteins with various levels of solubility to clarify the mechanism of aggregation and toxicity.

Acknowledgements

This work was supported in part by a Grant-in-Aid for Scientific Research on Priority Areas—Advanced Brain Science Project—from the Ministry of Education, Culture, Sports, Science and Technology, Japan, and by research grants from the Ministry of Health, Labor, and Welfare, Japan.

References

[1] M.M. Alba, R. Guigo, Comparative analysis of amino acid repeats in rodents and humans, Genome Res. 14 (2004) 549–554.
[2] Y. Oma, Y. Kino, N. Sasagawa, S. Ishiura, Intracellular localization of homopolymeric amino acid-containing protein expressed in mammalian cells, J. Biol. Chem. 279 (2004) 21217–21222.
[3] H.Y. Zoghbi, H.T. Orr, Glutamine repeats and neurodegeneration, Annu. Rev. Neurosci. 23 (2000) 217–247.
[4] R.L. Margolis, C.A. Ross, Expansion explosion: new clues to the pathogenesis of repeat expansion neurodegenerative diseases, Trends Mol. Med. 7 (2001) 479–482.
[5] L.Y. Brown, S.A. Brown, Alanine tracts: the expanding story of human illness and trinucleotide repeats, Trends Genet. 20 (2004) 51–58.
[6] J. Amiel, D. Trochet, M. Clement-Ziza, A. Munnich, S. Lyonnet, Polyalanine expansions in human, Hum. Mol. Genet. 13 (Suppl. 2) (2004) R235–R243.

[7] S.W. Davies, M. Turmaine, B.A. Cozens, M. DiFiglia, A.H. Sharp, C.A. Ross, E. Scherzinger, E.E. Wanker, L. Mangiarini, G.P. Bates, Formation of neuronal intranuclear inclusions underlies the neurological dysfunction in mice transgenic for the HD mutation, Cell 90 (1997) 537–548.
[8] M. DiFiglia, E. Sapp, K.O. Chase, S.W. Davies, G.P. Bates, J.P. Vonsattel, N. Aronin, Aggregation of huntingtin in neuronal intranuclear inclusions and dystrophic neurites in brain, Science 277 (1997) 1990–1993.
[9] M.Y. Sherman, A.L. Goldberg, Cellular defenses against unfolded proteins: a cell biologist thinks about neurodegenerative diseases, Neuron 29 (2001) 15–32.
[10] C.A. Ross, Polyglutamine pathogenesis: emergence of unifying mechanisms for Huntington's disease and related disorders, Neuron 35 (2002) 819–822.
[11] A. Michalik, C. Van Broeckhoven, Pathogenesis of polyglutamine disorders: aggregation revisited, Hum. Mol. Genet. 12 (Spec. No. 2) (2003) R173–R186.
[12] V. Shanmugam, P. Dion, D. Rochefort, J. Laganiere, B. Brais, G.A. Rouleau, PABP2 polyalanine tract expansion causes intranuclear inclusions in oculopharyngeal muscular dystrophy, Ann. Neurol. 48 (2000) 798–802.
[13] M.W. Becher, J.A. Kotzuk, L.E. Davis, D.G. Bear, Intranuclear inclusions in oculopharyngeal muscular dystrophy contain poly(A) binding protein 2, Ann. Neurol. 48 (2000) 812–815.
[14] S.E. Holmes, E. O'Hearn, A. Rosenblatt, C. Callahan, H.S. Hwang, R.G. Ingersoll-Ashworth, A. Fleisher, G. Stevanin, A. Brice, N.T. Potter, C.A. Ross, R.L. Margolis, A repeat expansion in the gene encoding junctophilin-3 is associated with Huntington disease-like 2, Nat. Genet. 29 (2001) 377–378 Erratum in: Nat. Genet. 30 (2002) 123.
[15] K.L. Moulder, O. Onodera, J.R. Burke, W.J. Strittmatter, E.M. Johnson Jr., Generation of neuronal intranuclear inclusions by polyglutamine-GFP: analysis of inclusion clearance and toxicity as a function of polyglutamine length, J. Neurosci. 19 (1999) 705–715.
[16] J. Rankin, A. Wyttenbach, D.C. Rubinsztein, Intracellular green fluorescent protein–polyalanine aggregates are associated with cell death, Biochem. J. 348 (2000) 15–19.
[17] S.E. Blondelle, B. Forood, R.A. Houghten, E. Perez-Paya, Polyalanine-based peptides as models for self-associated beta-pleated-sheet complexes, Biochemistry 36 (1997) 8393–8400.
[18] E. Scherzinger, R. Lurz, M. Turmaine, L. Mangiarini, B. Hollenbach, R. Hasenbank, G.P. Bates, S.W. Davies, H. Lehrach, E.E. Wanker, Huntingtin-encoded polyglutamine expansions form amyloid-like protein aggregates in vitro and in vivo, Cell 90 (1997) 549–558.
[19] C.C. Huang, P.W. Faber, F. Persichetti, V. Mittal, J.P. Vonsattel, M.E. MacDonald, J.F. Gusella, Amyloid formation by mutant huntingtin: threshold, progressivity and recruitment of normal polyglutamine proteins, Somat. Cell Mol. Genet. 24 (1998) 217–233.
[20] J.C. Dorsman, B. Pepers, D. Langenberg, H. Kerkdijk, M. Ijszenga, J.T. den Dunnen, R.A. Roos, G.J. van Ommen, Strong aggregation and increased toxicity of polyleucine over polyglutamine stretches in mammalian cells, Hum. Mol. Genet. 11 (2002) 1487–1496.
[21] E.A. Slee, C. Adrain, S.J. Martin, Serial killers: ordering caspase activation events in apoptosis, Cell Death Differ. 6 (1999) 1067–1074.
[22] J. Kyte, R.F. Doolittle, A simple method for displaying the hydropathic character of a protein, J. Mol. Biol. 157 (1982) 105–132.
[23] J.P. Taylor, J. Hardy, K.H. Fischbeck, Toxic protein in neurodegenerative disease, Science 296 (2002) 1991–1995.
[24] M. Bucciantini, E. Giannoni, F. Chiti, F. Baroni, L. Formigli, J. Zurdo, N. Taddei, G. Ramponi, C.M. Dobson, M. Stefani, Inherent toxicity of aggregates implies a common mechanism for protein misfolding diseases, Nature 416 (2002) 507–511.
[25] R. Kayed, E. Head, J.L. Thompson, T.M. McIntire, S.C. Milton, C.W. Cotman, C.G. Glabe, Common structure of soluble amyloid oligomers implies common mechanism of pathogenesis, Science 300 (2003) 486–489.
[26] N.F. Bence, R.M. Sampat, R.R. Kopito, Impairment of the ubiquitin–proteasome system by protein aggregation, Science 292 (2001) 1552–1555.
[27] M.S. Forman, V.M. Lee, J.Q. Trojanowski, 'Unfolding' pathways in neurodegenerative disease, Trends Neurosci. 26 (2003) 407–410.
[28] T. Nakagawa, H. Zhu, N. Morishima, E. Li, J. Xu, B.A. Yankner, J. Yuan, Caspase-12 mediates endoplasmic-reticulum-specific apoptosis and cytotoxicity by amyloid-beta, Nature 403 (2000) 98–103.
[29] Y. Kouroku, E. Fujita, A. Jimbo, T. Kikuchi, T. Yamagata, M.Y. Momoi, E. Kominami, K. Kuida, K. Sakamaki, S. Yonehara, T. Momoi, Polyglutamine aggregates stimulate ER stress signals and caspase-12 activation, Hum. Mol. Genet. 11 (2002) 1505–1515.
[30] H. Nishitoh, A. Matsuzawa, K. Tobiume, K. Saegusa, K. Takeda, K. Inoue, S. Hori, A. Kakizuka, H. Ichijo, ASK1 is essential for endoplasmic reticulum stress-induced neuronal cell death triggered by expanded polyglutamine repeats, Genes Dev. 16 (2002) 1345–1355.
[31] C. Hetz, M. Russelakis-Carneiro, K. Maundrell, J. Castilla, C. Soto, Caspase-12 and endoplasmic reticulum stress mediate neurotoxicity of pathological prion protein, EMBO J. 22 (2003) 5435–5445.

J. Biochem. **137**, 00–00 (2005)
DOI: 10.1093/jb/mvi058

Denervation Enhances the Expression of SHPS-1 in Rat Skeletal Muscle

Hiroaki Mitsuhashi[1], Ayumu Yoshikawa[1], Noboru Sasagawa[1], Yukiko Hayashi[2] and Shoichi Ishiura[1,*]

[1]Department of Life Sciences, Graduate School of Arts and Sciences, The University of Tokyo, 3-8-1 Komaba, Meguro-ku, Tokyo 153-8902; and [2]Department of Neuromuscular Research, National Institute of Neuroscience, National Center of Neurology and Psychiatry, Kodaira, Tokyo 187-8502

Received October 8, 2004; accepted February 4, 2005

SHPS-1 (Src homology 2 domain containing protein tyrosine phosphatase substrate 1) is a transmembrane glycoprotein containing three immunoglobulin-like motifs in its extracellular domain and immunoreceptor tyrosine-based inhibitory motifs (ITIM) that interact with SHP-2 (Src homology 2 domain containing protein tyrosine phosphatase-2) in its cytoplasmic region. SHPS-1 is highly expressed in brain, but at much lower levels in skeletal muscle. In this study, we found that the level of the SHPS-1 mRNA increases in rat skeletal muscle after denervation. Western blot analysis also confirmed the increase of SHPS-1 in denervated muscle. Moreover, it was found that the glycosylation of SHPS-1 is *N*-linked in a muscle-specific manner, and that this is altered upon innervation or denervation. Immunohistochemistry revealed SHPS-1 immunoreactivity at neuromuscular junctions (NMJs) under innervation, whereas immunoreactivity was observed extrasynaptically in muscle fibers after denervation. Our results indicate that the expression, glycosylation, and localization of SHPS-1 are strongly regulated by the nervous system, and that SHPS-1 may play an important role in denervated skeletal muscle.

Key words: denervation, glycosylation, neuromuscular junction, SHPS-1, skeletal muscle.

Abbreviations: AchRα, acetylcholine receptor α-subunit; ARPP16/19, cAMP-regulated phosphoprotein 16/19; BIT, brain immunoglobulin-like molecule with tyrosine-based activation motifs; α-BTX, α-bungarotoxin; ConA, Concanavalin A; Den, denervation; EDL, extensor digitorum longus; EGF, epidermal growth factor; GAPDH, glyceraldehyde-3-phosphate dehydrogenase; IGF-I, insulin-like growth factor-I; Inn, innervation; MAP kinase, mitogen-activated protein kinase; MFR, macrophage fusion receptor; NCAM, neural cell adhesion molecule; NMJs, neuromuscular junctions; PBS, phosphate-buffered saline; PVDF, polyvinylidene difluoride; SH2, Src homology 2; SHP-1/2, Src homology 2 domain containing protein tyrosine phosphatase-1/2; SHPS-1, Src homology 2 domain containing protein tyrosine phosphatase substrate 1; SIRP, signal-regulatory protein.

The differentiation of skeletal muscle is regulated by the nervous system. Neural innervation sends myotubes into myofibers. Skeletal muscle size, phenotype, and composition are also regulated, in part, by neural factors. Eliminating neural stimuli to muscle *via* peripheral nerve axotomy (denervation) impairs the highly differentiated state of skeletal muscle, leading to muscle atrophy. In addition, denervation results in changes in the expressions of muscle-specific genes, notably myogenic regulatory factors (MRFs) (*1–6*), the type II myosin heavy chain (MHC) isoform (*7*, *8*), and the acetylcholine receptor α subunit (AchRα) (*1*, *6*). For example, AchR is composed of five subunits including the ε-subunit ($\alpha\alpha\beta\delta\varepsilon$), and is restricted to neuromuscular junctions (NMJs) under innervation. But following denervation, the expressions of all AchR subunit genes increase, and the fetal type receptor, including a γ-subunit ($\alpha\alpha\beta\delta\gamma$), localizes throughout the sarcolemma. This implies that skeletal muscle after denervation reverts to a fetal, undifferentiated state both structurally and functionally. The identification and characterization of genes that are activated in denervated muscles might provide clues to the molecular mechanisms of muscle atrophy and differentiation.

SHPS-1 (Src homology 2 domain–containing protein tyrosine phosphatase substrate 1) (*9*), also known as SIRPα (*10*), BIT (*11*), MFR (*12*), and p84 neural adhesion molecule (*13*), is a transmembrane glycoprotein member of the immunoglobulin superfamily. SHPS-1 is abundant in certain neuronal and hematopoietic cells (*13–15*). The tissue distribution of SHPS-1 shows that it is abundant in the brain and spleen, and much less abundant in skeletal muscle (*9*, *16*). SHPS-1 has three immunoglobulin-like domains with multiple *N*-linked glycosylation sites in the extracellular region, and four YXX(L/V/I) motifs, which are putative tyrosine phosphorylation sites and binding sites for the Src homology 2 (SH2) domains of the protein-tyrosine phosphatases SHP-2 and SHP-1 (*9*, *10*), in the cytoplasmic region. Since the binding of SHP-2 to the tyrosine-phosphorylated cytoplasmic domain of SHPS-1 increases the protein tyrosine phosphatase activity of SHP-2 *in vitro* (*11*, *17*), it is thought that SHPS-1 regulates intracellular signaling by recruiting and activating SHP-2 near the plasma membrane. For example, overexpression of SIRPα1, the human homolog of SHPS-1, inhibits the insulin- or EGF-induced activation of MAP kinases and cell growth (*18*). Furthermore,

*To whom correspondence should be addressed. Tel/Fax: +81-3-5454-6739, E-mail: cishiura@mail.ecc.u-tokyo.ac.jp

expression of SHPS-1 has been shown to be down-regulated in fibroblasts transformed by various oncogene products (*19*). Thus SHPS-1 may be involved in growth factor–induced mitogenesis. In addition, Maile and Clemmons demonstrated that SHPS-1 recruits SHP-2 at the plasma membrane, leading to the dephosphorylation of insulin-like growth factor-I (IGF-I) receptor by SHP-2 in porcine aortic smooth muscle cells (*20*). Timms *et al.* (1999) reported that SHPS-1 acts as a scaffold for the assembly of multiprotein complexes (*21*). These observations suggest a role for SHPS-1 as a signal transducer in various cell types.

The extracellular region of SHPS-1 mediates cell–cell adhesion through the immunoglobulin-like domains. It has been reported that SHPS-1 contributes to macrophage multinucleation (*22*), T-cell activation (*23*), and the tethering of apoptotic cells to phagocytes (*24*) through cell adhesion. Recently, it was shown that SHPS-1 may be involved in the formation of filopodia between neuroblastoma cells (*25*). Thus, SHPS-1 may play a role in the modulation of signal transduction through cell–cell communication. However, its function *in vivo*, especially in skeletal muscle, is not fully understood.

To find genes involved in muscle atrophy or differentiation, we investigated differentially expressed genes in rat extensor digitorum longus (EDL) and soleus muscles after denervation by DNA microarray analysis followed by Northern blot analysis. The results revealed that SHPS-1 is remarkably up-regulated by denervation. In addition, we found that the degree of glycosylation and the localization of SHPS-1 are altered in denervated muscles. SHPS-1 does not interact with SHP-2 in denervated muscles. Taken together, SHPS-1 in skeletal muscle is modulated depending on neural influences, and could play an important role in denervated muscles. This is the first report on the characterization of SHPS-1 in skeletal muscle.

MATERIALS AND METHODS

Animals and Surgical Procedures—Adult male Wistar rats, 8 weeks of age and weighing approximately 250 g, were used in all experiments. Animals were anesthetized with nembutal (50 mg/kg), and the sciatic nerve on the right hindlimb was exposed. To maintain the denervated state for at least 2 weeks, a 1 cm segment of the sciatic nerve was surgically removed. At various time points, rats were deeply anesthetized and killed by decapitation. Extensor digitorum longus (EDL) and soleus muscles from both denervated (right) and innervated (left) legs were immediately removed, frozen in liquid nitrogen, and stored at –80°C

RNA Extraction and Northern Blot Analysis—Total RNA was extracted from frozen EDL and soleus with guanidium thiocyanate as described by Chomczynski and Sacchi (*28*). The total RNA in each sample (10–20 μg) was electrophoresed in a 1.0% agarose gel containing formaldehyde and then transferred to a nylon membrane (Biodyne B, KPL). The membranes were hybridized in hybridization solution (ULTRAhyb, Ambion) according to the manufacturer's instructions with ^{32}P-labeled cDNA fragments encoding mouse SHPS-1 (NCBI Genbank #D87967, 1626–1993), mouse SHP-2 (NCBI Genbank #NM_011202, 1261–1849), human AchRα(NCBI Genbank #NM_000079, 375–887), and human glyceraldehyde-3-phosphate dehydrogenase (GAPDH) (NCBI Genbank #BC023632, 369–717). Autoradiographic signals were analyzed and quantified by a Bioimaging Analyzer System (BAS, Fujifilm).

DNA Microarray Analysis—DNA microarray analysis was performed with Atlas Glass Array Rat 1.0 (CLONTECH) containing 1,090 kinds of gene-specific 80 bp oligonucleotides.

Western Blot Analysis and Deglycosylation—Anti–SHPS-1 rabbit polyclonal antibodies were purchased from Upstate Biotechnology Lake Placid, NY, USA). Anti–SHP-2 mouse monoclonal antibodies were purchased from Transduction Laboratories (Lexington, KY, USA).

Innervated and denervated muscles and brain from rats were homogenized on ice in 2 ml of homogenization buffer [50 mM Tris-HCl (pH 7.5), 1 mM EDTA, 150 mM NaCl, 1% Nonidet P-40 containing 50 mM sodium fluoride, 1 mM phenylmethylsulfonyl fluoride, 1 mM sodium orthovanadate and 0.1% inhibitor mix (WAKO)] with a polytron homogenizer (HITACHI KOUKI). The homogenates were centrifuged at 1,000 × *g* for 2 min at 4°C, and the supernatants were collected. The supernatants were solubilized by rotation for 1 h at 4°C, and centrifuged at 10,000 × *g* for 15 min at 4°C. The resulting supernatants were subjected to immunoblot analysis. Protein concentration was determined using a DC protein assay kit (BIO-RAD). Approximately 20 μg of total homogenates were subjected to 7.5% SDS-PAGE and then transferred to PVDF membranes (finetrap NT-32, Nihon Eido) using a semi-dry electroblotting apparatus. The membranes were blocked for 1 h with 5% non-fat dry milk in phosphate-buffered saline (PBS) containing 0.05% Tween-20 at room temperature. The membranes were incubated with primary antibodies (anti–SHPS-1 at 1:1,000; anti–SHP-2 at 1:5,000) for 30 min at 37°C or overnight at 4°C. The primary antibodies were detected with anti–rabbit IgG horseradish peroxidase–conjugated antibodies (1:5,000) or anti–mouse IgG horseradish peroxidase–conjugated antibodies (1:5,000) for 30 min at 37°C, and then the membranes were incubated in freshly prepared chemiluminescence buffer [100 mM Tris-HCl (pH 8.5), 1.25 mM luminal, 0.2 mM *p*-coumaric acid, 0.009% H_2O_2] for 1 min at room temperature, and exposed to film (hyperfilm™ ECL, Amersham Biosciences).

To examine the glycosylation of SHPS-1, homogenates were boiled in the presence of 1% SDS and 1% 2-mercaptoethanol for 3 min and then subjected to deglycosylation with 2 U/ml of *N*-glycosidase F (Roche) in 50 mM Tris-HCl (pH 7.5) containing 50 mM EDTA, 1% 2-mercaptoethanol, and 1% TritonX-100 for 20 h at 37°C.

Concanavalin A Sepharose Precipitation—Innervated and denervated muscles were homogenized on ice in 2.5 ml of homogenization buffer [50 mM Tris-HCl (pH 7.5), 5 mM EDTA, 5 mM EGTA, 50 mM NaCl, containing 50 mM sodium fluoride, 1 mM phenylmethylsulfonyl fluoride, 1 mM sodium orthovanadate and 0.1% inhibitor mix (WAKO)] with a polytron homogenizer (HITACHI KOUKI). The homogenates were centrifuged at 1,000 × *g* for 2 min at 4°C, and the supernatants were collected. The supernatants were solubilized by rotation for 1 h at 4°C, and centrifuged at 100,000 × *g* for 60 min at 4°C. The

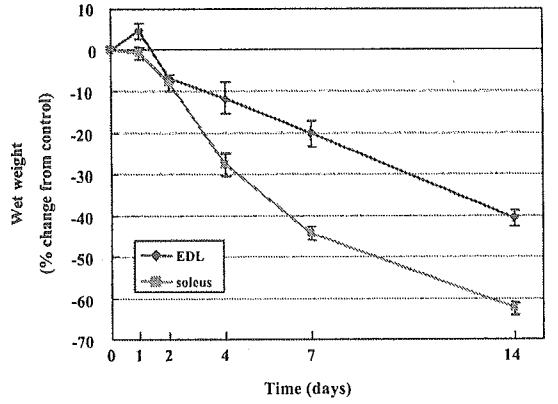

Fig. 1. **Time course of weight loss of rat EDL and soleus muscles after denervation.** Values are means ± SE; n = 7.

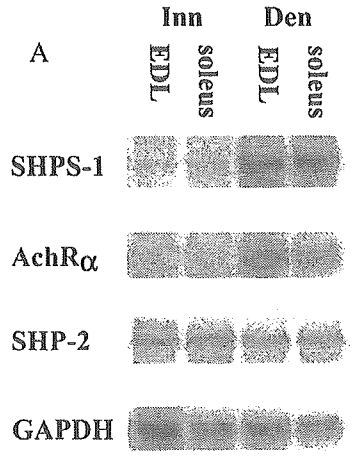

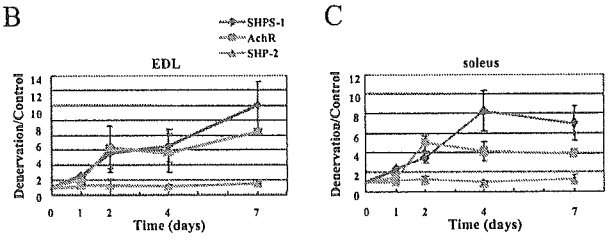

Fig. 2. **Northern blot analysis of SHPS-1, AchRα, and SHP-2.** (A) Bands are the signals of SHPS-1, AchRα and SHP-2 mRNA in innervated (Inn) and 7-day denervated (Den) EDL and soleus muscles. The ratios of mRNA expression of three genes to GAPDH in EDL (B) and soleus (C) muscles 1, 2, 4, and 7 days after denervation are shown. Values are means ± SE; n = 3.

resulting supernatants were removed, and the pellets were suspended in 0.8 ml membrane solubilization buffer [20 mM Tris-HCl (pH 7.5), 1% Triton X-100, 150 mM NaCl, 1 mM $MgCl_2$ containing 50 mM sodium fluoride, 1 mM phenylmethylsulfonyl fluoride, 1 mM sodium orthovanadate and 0.1% inhibitor mix (WAKO)]. The suspensions were centrifuged at 100,000 × g for 60 min at 4°C, and the resulting supernatants were referred to as the solubilized membrane fractions. The amount of total protein in the solubilized membrane fractions was standardized using a DC protein assay kit (BIO-RAD) before Concanavalin A (ConA) Sepharose precipitation, and the solubilized membrane fractions were incubated with 50 μl ConA Sepharose beads (Amersham Biosciences) overnight at 4°C. The beads were then washed three times with 0.5 ml membrane solubilization buffer, resuspended in SDS sample buffer [50 mM Tris-HCl (pH 6.8), 2% SDS, 6% 2-mercaptoethanol, 1% glycerol (v/v), 0.1% bromophenol blue], and boiled for 3 min at 100°C.

Immunohistochemistry—Tissues were excised, frozen in cold iso-pentane, and sectioned with a cryostat (6 μm). The sections were fixed in 4% paraformaldehyde in PBS for 15 min at 4°C. After pre-incubation with PBS containing 2% bovine serum albumin and 5% heat-inactivated normal goat serum, the sections were incubated with anti–SHPS-1 antibody at 1:250 or anti–SHP-2 antibody, C-18, at 1:250 (Santa Cruz Biotechnology) overnight at 4°C, and then incubated with anti-rabbit IgG antibody–conjugated Oregon green (Molecular Probes) at 1:500 and 2 μg/ml α-bungarotoxin–conjugated rhodamine (Molecular Probes) for 30 min at room temperature. Sections were observed under a fluorescence microscope (OLYMPUS IX70, OLYMPUS).

Statistical Analysis—All values are expressed as mean ± SE. Statistical analysis was performed by Student's t-test.

RESULTS

Weight Loss of Rat EDL and Soleus Muscles after Denervation—The decreases in the wet weights of the EDL and soleus muscles with time after denervation are shown in Fig. 1. The wet weights of both muscles were unchanged 1 day after denervation and started to decrease constantly after 2 days. Soleus muscles decreased in wet weight at a faster rate than EDL muscles after 4 days. Finally, soleus muscles decreased to 37.4 ± 1.5% (n = 7) of their initial weight and EDL muscles to 59.1 ± 1.9% (n = 7) of their initial weight 2 weeks after denervation.

Expression of SHPS-1 mRNA in Denervated Muscles—To identify novel genes involved in the changes in muscles after denervation, we compared mRNA expression in EDL and soleus muscles 7 days after denervation with that in control muscles using DNA microarrays (data not shown). The expressions of several genes were shown to be increased in denervated muscles, and Northern blot analysis was performed for these genes. We found *SHPS-1* to be remarkably up-regulated in both EDL and soleus muscles 7 days after denervation (Fig. 2A). We also found that *AchRα* was dramatically up-regulated after denervation.

To further analyze the expression of these genes, we quantitated the expressions of SHPS-1, SHP-2 and AchRα using mRNA prepared from denervated muscles 1 to 7 days after denervation (Fig. 2, B and C). In EDL muscles, the expressions of SHPS-1 and AchRα increased constantly after denervation, reaching 12-fold (SHPS-1) and 8.5-fold (AchRα) elevations, respectively, after 7 days. The expression of SHP-2, which is known to interact with SHPS-1, did not change after denervation. In

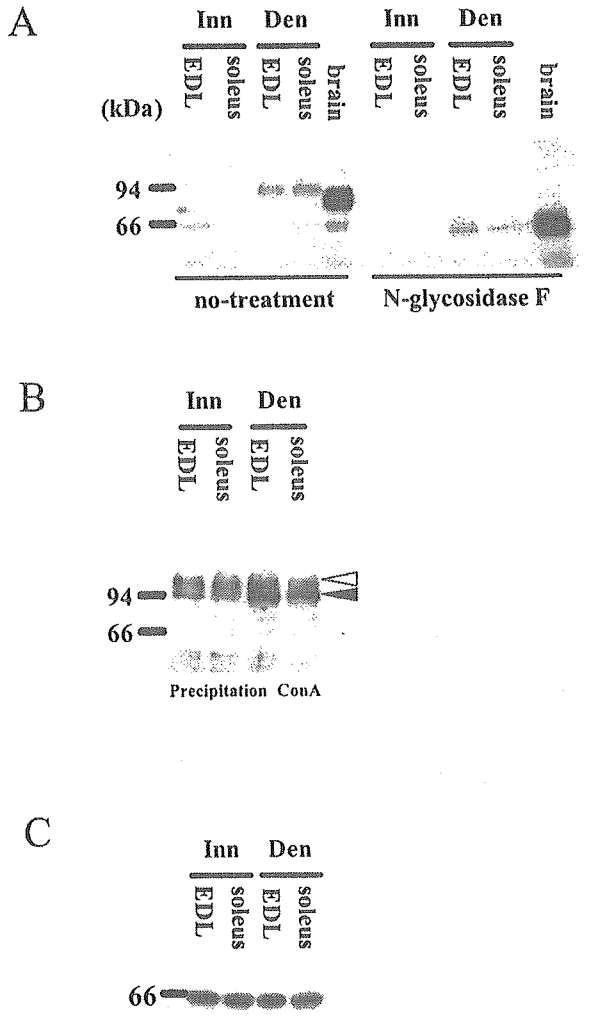

Fig. 3. **Western blot analysis of SHPS-1 and SHP-2 in rat skeletal muscles.** (A) Lysates were prepared from innervated (Inn) and 7-day denervated (Den) muscles, and immunoblotted with anti–SHPS-1 antibody. *N*-glycosidase F treatment was performed as described in "MATERIALS AND METHODS." (B) Solubilized membrane fractions of innervated (Inn) and denervated (Den) muscles were incubated with Con A-Sepharose beads. The proteins bound to Con A-Sepharose were separated by SDS-PAGE and immunoblotted with anti–SHPS-1 antibody. Two major bands were detected, "upper" (open arrowhead) and "lower" (filled arrowhead) SHPS-1. (C) Lysates from innervated (Inn) and 7-day denervated (Den) muscles were immunoblotted with anti–SHP-2 antibody.

soleus muscles, the expression of SHPS-1 increased constantly from 1 to 4 days after denervation, and remained elevated thereafter (a 7-fold increase after 7 days). The expression of AchRα increased rapidly to a 5-fold higher level after 2 days, and then remained high (a 4-fold elevation after 7days). The expression of SHP-2 was also unchanged in soleus muscles.

Glycosylation of SHPS-1 in Innervated and Denervated Muscles—To confirm that the level of the SHPS-1 protein increases in denervated muscles, Western blot analysis was performed with anti–SHPS-1 antibody. As shown in Fig. 3A (left), specific bands with molecular sizes of about 94 kDa were detected in denervated muscles, but not in innervated muscles. In rat brain, the antibody detected a band of about 90 kDa. Because it was thought that these differences in molecular size result from differential glycosylation, we examined shifts in the bands after deglycosylation with *N*-glycosidase F. Deglycosylation converted the molecular sizes of the bands in both denervated muscle and brain samples to about 65 kDa (Fig. 3A, right). Furthermore, we precipitated SHPS-1 with Concanavalin A (Con A) Sepharose. Con A precipitation revealed that a small amount of SHPS-1 protein exists in innervated muscles. Another SHPS-1 species with a molecular mass greater than 94 kDa ("upper" SHPS-1) was detected in both innervated and denervated muscles (Fig. 3B). It was thought that this is the more glycosylated form of SHPS-1. These results indicate that the SHPS-1 protein is expressed in both innervated and denervated muscles and modified in two distinct manners, and that the expression of a form of about 94 kDa ("lower" SHPS-1) increases after denervation, as in the case of the SHPS-1 mRNA. SHP-2 did not undergo any change in denervated muscles (Fig. 3C).

Localization of SHPS-1 in Innervated and Denervated Muscles—To examine whether SHPS-1 is expressed in muscle fibers, we observed EDL and soleus muscle sections immunostained with anti–SHPS-1 antibody. Immunoreactivity was observed as a few small dots in innervated muscles, but diffusely in the plasma membranes of muscle fibers after denervation (Fig. 4). While most fibers were immunoreactive in EDL muscles after denervation (Fig. 4B), only some fibers were immunoreactive in soleus muscles, showing patch-like staining (Fig. 4F). Moreover, anti–SHPS-1 immunoreactivity was also observed at neuromuscular junctions under innervation (Fig. 5A). This localization was confirmed by double-staining with anti–SHPS-1 antibody and rhodamine-conjugated α-bungarotoxin (α-BTX) (Fig. 5C). Since anti–SHPS-1 antibody and α-BTX stainings colocalized in denervated muscles, it was confirmed that anti–SHPS-1 immunoreactivity, like AchRs, localizes on plasma membranes in muscle fibers (Fig. 5, B and D).

We also stained muscle sections with anti–SHP-2 antibody. Immunoreactivity was observed in the cytoplasm in both innervated and denervated muscles (Fig. 6). SHP-2 was not localized at neuromuscular junctions. These observations imply that SHP-2 is not regulated by innervation.

DISCUSSION

Previously, we found by DNA microarray analysis that another gene, ARPP16/19, is highly up-regulated in denervated rat muscle (27). However, this protein is a cytoplasmic adaptor and no physiological role was implicated. In this report, we provide the first demonstration that SHPS-1 is highly expressed in rat denervated skeletal muscles. We also show that the expression, glycosylation, and localization of SHPS-1 are altered after denervation. In contrast, SHP-2 does not change its expression or localization after denervation. These results suggest that SHP-2 is not involved in SHPS-1 function in denervated muscles. Taken together, SHPS-1 and SHP-2 may be regulated in different pathways in rat skeletal muscles.

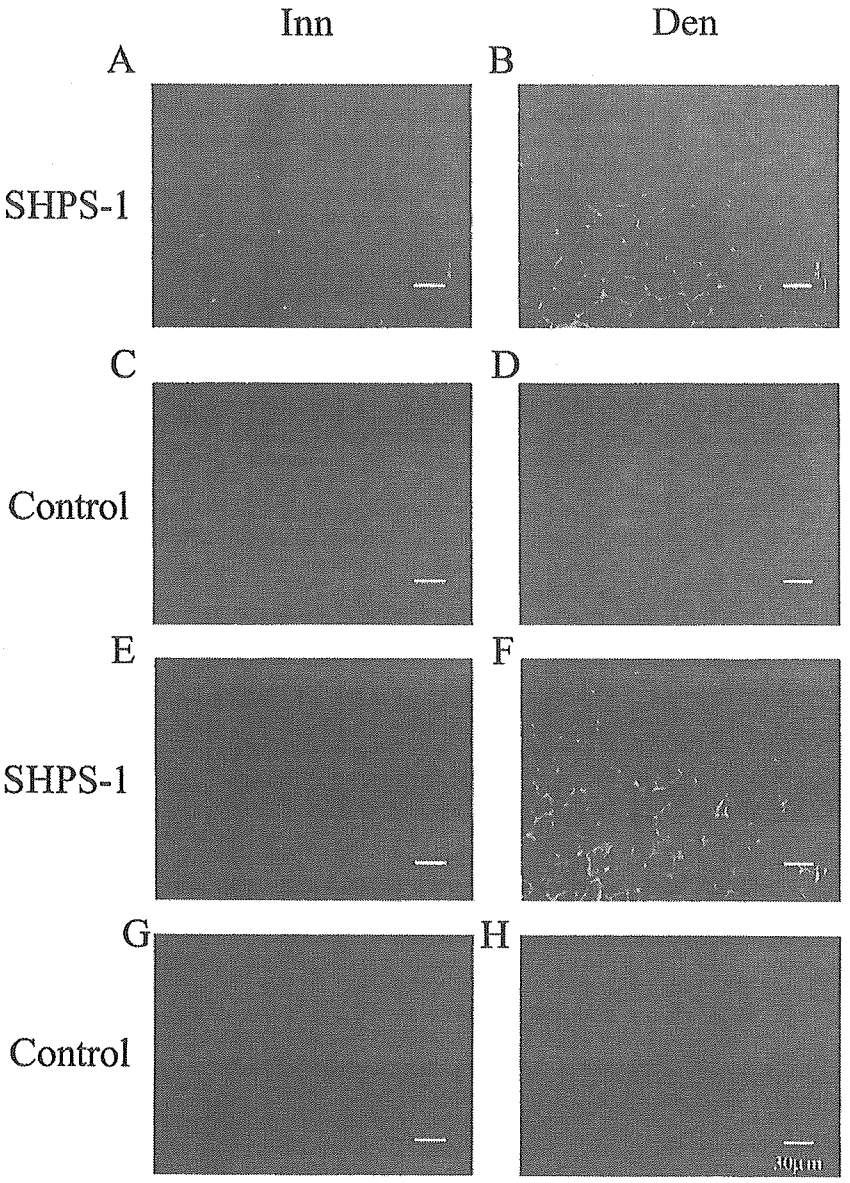

Fig. 4. **Localization of SHPS-1 in rat skeletal muscles.** Cross-sections of innervated (A, E) and 7-day denervated (B, F) muscles stained with anti–SHPS-1 antibody. A series of sections was stained without a primary antibody as a control (C, D, G, H). (A–D) EDL, (E–H) soleus ; Bar = 30 μm

We have demonstrated that the expression of SHPS-1, although very low in innervated muscles, increases in denervated muscle in a manner similar to that of AchRα. AchR is one of the most important cation channels for neuromuscular transmission. It is concentrated at NMJs, and is remarkably up-regulated after denervation (*28*). It is thought that this is a compensation mechanism for a loss of acetylcholine. Often, other proteins induced by denervation are up-regulated at far lower rates than the AchRα, but the SHPS-1 mRNA increases remarkably (Fig. 2). This implies that the increase in the expression of SHPS-1 may compensate for a loss of neural stimuli, and that SHPS-1 may play a role in innervation.

The levels of SHPS-1 and AChRαmRNA are relatively low under innervation and rise rapidly following denervation. In addition, we have observed that SHPS-1 immunoreactivity localizes at NMJs in innervated muscles and throughout the plasma membrane in denervated muscles. Although AchR and its interacting proteins, MuSK and rapsyn, are expressed at low levels and are restricted to NMJs under innervation, denervation induces increases in their expressions, and their localization becomes extrasynaptic (*29–31*). NCAM and BEN/SC1/DM-GRASP, members of the immunoglobulin superfamily, also show these alterations (*32–36*). NCAM is thought to play an important role in neurogenesis through cell–cell contacts (*37*, *38*). In recent studies, it was reported that SHPS-1 binds to CD47 via its extracellular domain, and this interaction is implicated in synapse formation or maintenance (*39*). Taken together, it is possible that SHPS-1 is involved in nerve–muscle cell interaction.

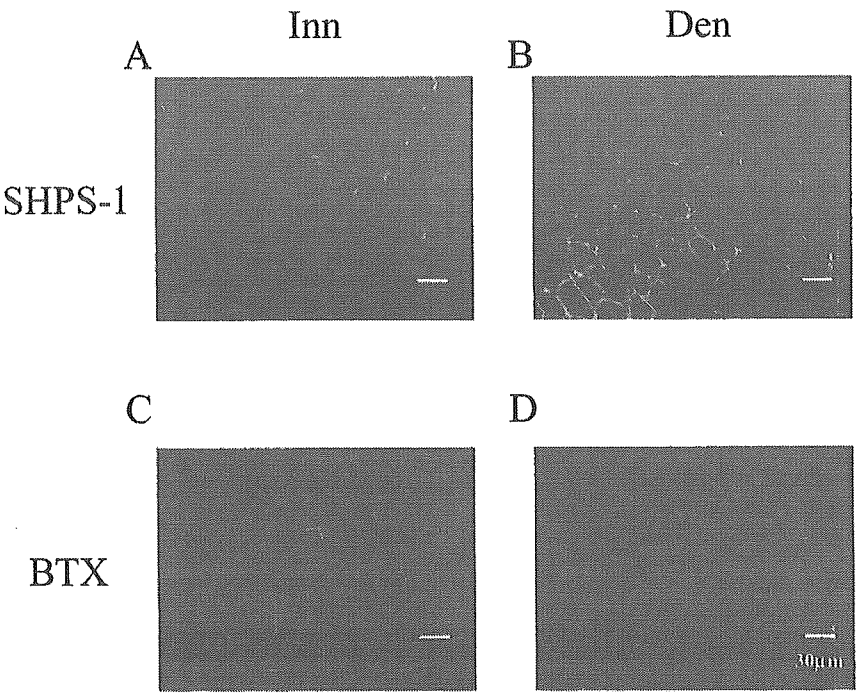

Fig. 5. **Co-localization of SHPS-1 and AchR in innervated and denervated muscles.** Cross-sections of innervated and 7-day denervated EDL muscle were double-stained with anti–SHPS-1 antibody (A, B) and rhodamine-conjugated α-bungarotoxin (BTX) (C, D). (A, C) innervated (B, D) denervated; Bar = 30 μm.

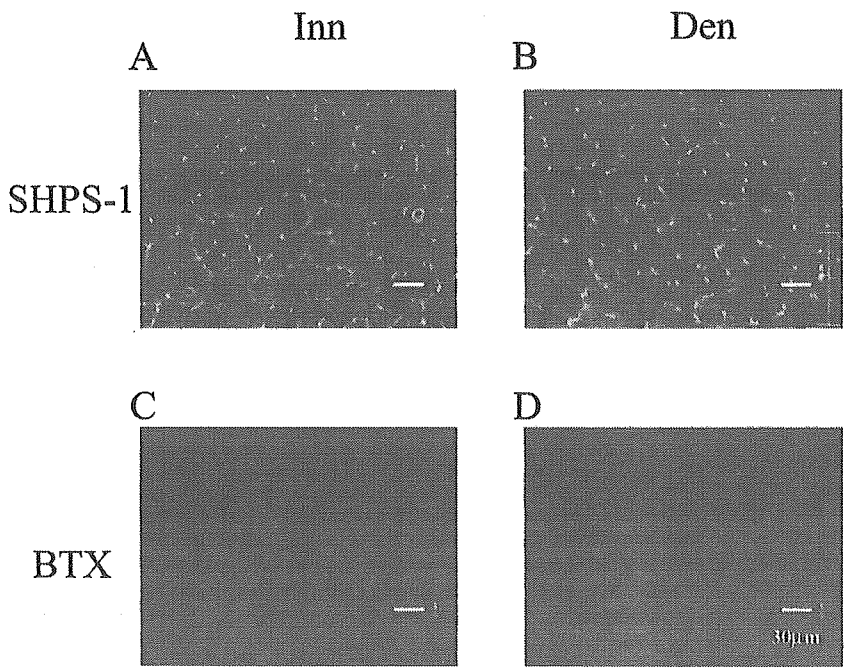

Fig. 6. **Immunohistochemistry of SHP-2 in EDL muscle.** Cross-sections of innervated and 7-day denervated EDL muscle were stained with anti–SHP-2 antibody (A, B). A series of sections was stained without a primary antibody as a control (C, D). (A, C)innervated (B, D)denervated ; Bar = 30 μm.

The rates of increase of SHPS-1 expression and immunoreactivity with the anti–SHPS-1 antibody differ slightly between EDL and soleus muscles. These differences may be due to the difference in fiber types. Muscle atrophy progresses at different rates in EDL and soleus muscles. Thus, differences in the nature of the muscle fibers might account for the small difference in SHPS-1 expression.

The glycosylation of SHPS-1 is regulated in tissue-specific manner, and the isoform in skeletal muscle is different from that in brain. Moreover, two distinct isoforms with different affinities for Con A exist in skeletal muscle, and the expression of only one form increases after denervation. Generally, glycosylation modulates the adhesion activity of glycoproteins, and it is reported that the aberrant *N*-glycosylation of SHPS-1 impairs its abil-